Level structure of ^{154}Ho

Chang-Bum Moon,[1,*] Tetsuro Komatsubara,[2,3] and Kohei Furuno[2]
[1]*Hoseo University, Asan, Chungnam 336-795, Korea*
[2]*Research Facility Center for Pure and Applied Science, University of Tsukuba, Ibaraki 305-8577, Japan*
[3]*Rare Isotope Science Project, Institute for Basic Science, Daejeon 305-811, Korea*
(Received 1 August 2013; revised manuscript received 18 September 2013; published 8 October 2013)

The excited states of the odd-odd ^{154}Ho nucleus have been studied by using in-beam γ-ray spectroscopy with the ^{141}Pr (^{16}O, $3n$) ^{154}Ho reaction at $E_{\rm lab} = 75$ MeV. The beam was provided by the 12UD Pelletron accelerator at the University of Tsukuba. In this work, the complicated decay pattern of low energy transitions just above the $T_{1/2} = 3.10$ min isomer have been established. In addition, a number of new states and γ-ray transitions, especially those associated with energetically favored band termination, have been observed for the first time in ^{154}Ho. A negative collective band and its signature partner built on the 11^- level are interpreted as being based on the $\pi h_{11/2} \otimes \nu i_{13/2}$ configuration. A positive band built on the 10^+ level is based on the $\pi h_{11/2} \otimes \nu h_{9/2}$ configuration while another positive band built on the 9^+ level is being associated with the $\pi h_{11/2} \otimes \nu f_{7/2}$ configuration. An energetically favored level $J^\pi = 19^-$ can be interpreted as being attributed to the $\pi h_{11/2} \otimes \nu i_{13/2}$ configuration coupled to the 8^+ state in neighboring core ^{152}Dy, namely, a four-quasiparticle alignment based on the $[\pi h_{11/2} \nu i_{13/2}]_{11^-} \otimes [\nu(h_{9/2} f_{7/2})]_{8^-}$ configuration. Another energetically favored state at $J^\pi = 27^-$ is assigned the six-quasiparticle $[\pi(h_{11/2})^3]_{27/2^-} \otimes [\nu(f_{7/2} h_{9/2} i_{13/2})]_{27/2^-}$ configuration.

DOI: 10.1103/PhysRevC.88.044308 PACS number(s): 21.10.Re, 23.20.Lv, 25.70.Gh, 27.70.+q

I. INTRODUCTION

For dysprosium ($Z = 66$) and erbium ($Z = 68$) nuclei, the properties of yrast spin states were found to be very sensitive to small changes in neutron number N, giving rise to different structural phenomena, such as shape coexistence, large variations of the quadrupole collectivity (phase transition), and low-lying intruder states. For example, Dy and Er isotopes [1–6] represent spherical singles states, vibrational states, and rotational states from $N = 80$ to $N = 92$ as shown in Fig. 1. Here the values of the ratios of the first 4^+ and 2^+ states, $R = E(4^+)/E(2^+)$, convey nuclear structural information: R evolves from <2 for spherical nuclei, through 2 for vibrational structures, to 3.33 for well deformed axial rotors [3,7]. The ^{152}Dy [4] and the ^{154}Er [6] nuclei with $N = 86$ apparently show an intermediate character, depicting collective vibrational characteristics as expected for near-spherical nuclei with a small deformation, $\epsilon_2 \approx 0.14$ [8].

In this region, the neutron intruder $\nu i_{13/2}$ orbital can be easily occupied by a neutron quasiparticle, thereby driving the shape into prolate deformation because of its fast downsloping in energy. Many collective $\Delta J = 2$ bands observed in odd-N Dy and Er nuclei have been identified as being built on the $\nu i_{13/2}$ orbital while the ground band consisting of yrast states in odd-even Ho has been built on states based on the proton $\pi h_{11/2}$ orbital [9–14]. It is expected, therefore, that doubly odd nuclei in this region have negative-parity collective bands based on the configuration of the proton intruder $h_{11/2}$ orbital coupled to the neutron intruder $i_{13/2}$ orbital. Indeed, band structures built on $\pi h_{11/2} \otimes \nu i_{13/2}$ as well as other combinations of quasiprotons and quasineutrons have been commonly observed in the odd-odd Ho nuclei [15–19]. Thus odd-odd Ho nuclei provide a good scope to study the role of proton-neutron interaction and its influence on both collective motion and single particle motion. A single quasiparticle in a high-j shell generates a torus-shaped density distribution which induces an oblate shape of the nucleus, with the spin along the symmetry axis. Such quasiparticle alignments result in energetically favored states (yrast states) and give rise to single particle energy structures in Dy, Ho, and Tb around $N = 86$ [9,10,20].

Detailed studies in the case of odd-odd nuclei, however, are very difficult both experimentally and theoretically due to the complexity of their excitation mechanism. γ-ray spectroscopic studies for the excited states of ^{154}Ho were previously made [15,20]; however, detailed level properties have not appeared until now. In the present work, we have clearly established the complicated low-lying energy transitions just above the 3.10 min isomer and extended the known levels up to higher spins.

II. EXPERIMENTAL PROCEDURES

The excited states of ^{154}Ho have been investigated by using in-beam γ-ray spectroscopy with the ^{141}Pr(^{16}O, $3n$)^{154}Ho reaction at a beam energy of 75 MeV. The beam was provided by the 12UD tandem accelerator at the University of Tsukuba in Japan. The target was a self-supporting foil of natural Pr with a 2.7 mg/cm^2 area density. The γ-ray spectra were taken with 11 high-purity (HP) Ge detectors with BGO($Bi_4Ge_3O_{12}$) anti-Compton shields (ACS). One of them was the LEPS (low energy photon spectrometer) detector to ensure sensitivity for important low-energy transitions at the bottom parts of γ-ray cascades. The efficiencies and energy calibrations were performed with a standard γ-ray ^{152}Eu source. The intrinsic resolution of the HP Ge detectors was typically about 2.2 keV for a 1.33-MeV γ ray. Approximately 90 million events in which two or more HP Ge detectors registered in prompt coincidence were collected. In the offline analysis,

*cbmoon@hoseo.edu

 ©2013 American Physical Society

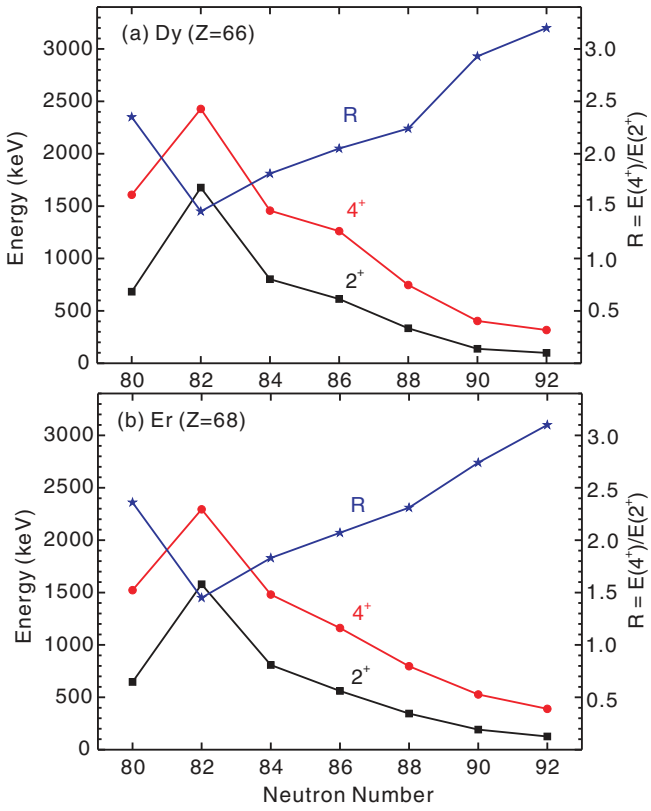

FIG. 1. (Color online) Systematics for the first excited 2^+ and 4^+ levels in Dy (upper part) and in Er (lower part) isotopes as a function of neutron number. For a structural comparison the values of their ratios, $R = E(4^+)/E(2^+)$, are plotted. Data are taken from the evaluated nuclear structure data file (ENSDF) [2].

the coincidence data were recalibrated to 0.5 keV/channel for Ge and 0.25 keV/channel for the LEPS and sorted into 4096 by 4096 channel triangular matrices. The γ-ray coincidence relations were established by setting gates on the photopeaks of the individual transitions and projecting the coincidence spectra. Gates were also put on the background in the vicinity of the photopeaks to remove contributions due to the background below the photopeaks of the gating transitions. Multipolarity information was extracted from the data by using the method of directional correlation of oriented states (DCO ratios). To this end, the coincidence events were sorted into an asymmetric matrix with energies of γ rays detected in five detectors at 37° (or 143°) along one axis and energies of γ rays detected in five detectors at 79° (or 101°) along the other axis. The intensities of $I_\gamma(37°)$ and $I_\gamma(79°)$ used to determine the DCO ratio, $R_{\rm DCO} = I_\gamma(37°)/I_\gamma(79°)$, for the transitions of interest were extracted from spectra obtained by setting gates on the 37° and 79° axes of the asymmetric matrix. In general, the DCO ratios were determined by setting gates on transitions in the band sequence preceding or following the transition of interest. For the γ-ray transitions with known multipolarities, when both the gating and the observed transitions are stretched and have the same multipolarity, the DCO ratio is $R_{\rm DCO} \approx 1$; if the gate is set on a stretched quadrupole (dipole) transition and one looks at a stretched dipole (quadrupole) transition, the DCO ratio is $R_{\rm DCO} \approx 0.6(1.8)$. If the gate is on a stretched quadrupole transition and one observes a mixed dipole-quadrupole transition with $\Delta J = 1$, the $R_{\rm DCO}$ ratios depend on the $\delta(M1/E2)$ mixing parameter and range from 0.5 for $\delta = -1.0$ to 2.5 for $\delta = 1.0$. As the gating transition, the stretched quadrupole γ rays were chosen. Thus, the multipolarities of all other transitions with available DCO ratios have been extracted in the present work.

III. LEVEL SCHEME OF ^{154}Ho

Figure 2 shows the level scheme built on the 8^+ isomer with $T_{1/2} = 3.10$ min in ^{154}Ho. An expanded view of low lying levels is also shown in the same figure for clarity. The ordering of the γ-ray transitions was determined from coincidence relationships and relative intensities. Information on γ-ray multipolarities was obtained from the DCO ratios mentioned in the previous section. Because of the presence of overlapping γ-rays from the neighboring channels ($4n$, $p2n$, etc.) in the total projection spectrum, the relative intensities were obtained from the sum gated spectrum of specific transitions in ^{154}Ho. Our results for γ-ray transitions, intensities, excitation energies, DCO ratios, and spin assignments for ^{154}Ho are summarized in Tables I and II. Here, the energy of the 8^+ isomer is set to 0 for reference since its excitation energy remains uncertain. It should be noted, however, there are indications that this decaying isomer is located at 320 keV [1,21,22] or 238 ± 30 keV [23] above the ground state.

The ground state of ^{154}Ho is known to be $J^\pi = 2^-$ with a half-life of 11.76 min [1]. In the present work, no evidence for the transitions feeding the ground state has been obtained in coincidence spectra associated with the Ho characteristic x-ray gate. Since the present reaction is expected to populate preferentially the higher spin states, low-lying spin states built on the ground state of 2^- may not be populated with appreciable yield. For studies of odd-odd nuclei, we encounter the well known difficulties resulting from the existence of low-energy γ-ray transitions which are attenuated and are often below observation sensitivity thresholds for typical experiments. In the current work, the LEPS detector plays a role in ensuring sensitivity for low-energy transitions at the bottom parts of γ-ray cascades in ^{154}Ho. Figure 3 displays a coincidence spectrum for the characteristic γ rays from the excited states in Ho nuclei when gates are set on the 47-keV Ho $K\alpha_1$ x ray. We can see that most intense γ rays in coincidence with the 47-keV Ho x ray come from the transitions in the excited states of ^{154}Ho.

Low-lying states below the 393-keV level are very complicated as showing correlations with unobserved low-energy transitions and crossover ones. Thanks to the LEPS detector, as Fig. 4(a) shows, a 54.3-keV γ ray could be nicely separated from the 53.9-keV Ho x ray, and thus by the coincidence relationships between the corresponding transitions the 54.3 transition is definitely placed on the states in ^{154}Ho. The 20.9-keV level could be established by a relation between the 339.3-keV transition and three parallel cascading transitions, namely, 318.4-20.9, 54.3-264.1-20.9, and 54.3-71.7-192.4-20.9, the sum of which corresponds to 339.3 keV. The 18.8-keV level should exist as well because of a relationship between the 285.0-keV transition and the 266.2-18.8 (=285.0 keV)

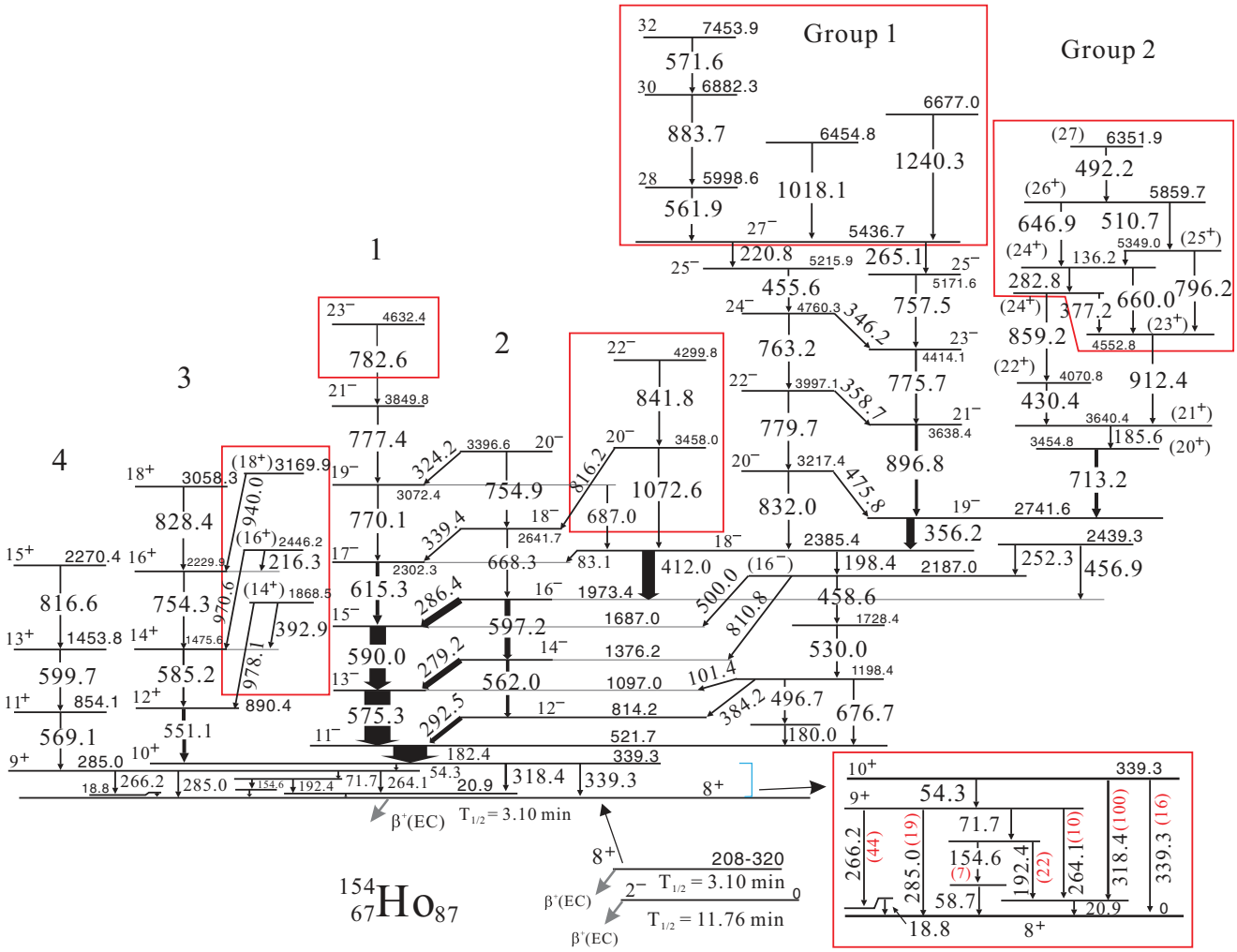

FIG. 2. (Color online) The level scheme built on the isomeric 8^+ state of ^{154}Ho deduced from the ^{141}Pr (^{16}O, $3n$) ^{154}Ho reaction at a beam energy of 75 MeV. Energies are given in keV and level energies are expressed relative to the 8^+ isomer. The widths of the arrows are proportional to the relative intensities of γ-ray transitions above the 10^+ state at 339.3 keV. The relative intensities, however, for the transitions between the 10^+ state and the isomer are denoted by numbers. Tentative spin and parity assignments are given in parentheses. The new levels and new γ-ray transitions are marked by the red (gray) line boxes.

cascading transition. The 285-keV transition is also equal to the sum energy consisting of another set of parallel cascading transitions, namely, 71.7-154.6-58.7 keV [see Fig. 4(b)]. These two, 20.9 and 18.8 keV, γ rays are too low in energy as well as too weak in intensity due to internal electron conversion to be detected by the present LEPS detector capacity.

Figure 5 shows representative γ-ray spectra in coincidence with the transitions assigned to ^{154}Ho. Bands 1 and 2 built on the $J^\pi = 11^-$ were most strongly populated up to $J^\pi = 16^-$ and were already known in previous works [15,20]. The yrast nature of the states and the strong intraband transitions provide evidence that bands 1 and 2 are signature partners. The lowest transitions in bands 3 and 4 were populated with intensities of about 14% and about 6.5% of that of band 1, respectively. The spin assignments for the bandheads of bands 1 to 4 are consistent with those for the similar collective bands observed in heavier odd-odd isotopes [16–19] and odd-odd ^{152}Tb [24,25].

The spin-parity assignment for the 18^- level at 2385.4 keV was made by the 412.0-keV transition which shows a quadrupole $\Delta J = 2$ type in the DCO ratios and thus it was assigned to have an $E2$ transition. The spin-parity for the 27^- level at 5436.7 keV was proposed with the $E2$ assignment of the 221-keV γ ray that has a stretched $\Delta J = 2$ type (see Fig. 5).

In the DCO spectra, the 713-keV transition feeding the 19^- state at 2741.6 keV indicates a $\Delta J = 1$ type character but DCO ratios are somewhat different from those of other transitions with $M1$ dipole nature. The DCO ratios of the 713-keV transition were around 0.56 while those for the $M1$ transitions, such as 279.2, 286.4, and 356.2 keV, were 0.65 to 0.69 when gating set on the known stretched quadrupole transitions. Such a high asymmetric angular distribution indicates that the 713-keV transition very likely has a pure $E1$ character. Thus we propose that the 3454.8-keV level should be a positive-parity state, namely, $J^\pi = 20^+$.

TABLE I. γ-ray energies, relative intensities, excitation energies, DCO ratios, and spin-parity assignments for the levels between the 10^+ at 339.3 keV and the 8^+ isomer in ^{154}Ho. The excited energy of the 8^+ isomer is set to 0 for reference. The relative intensities are deduced from a gate spectrum in coincidence with a 182.4 keV transition. The electron conversion effect was not considered.

E_γ [a]	I_γ [b]	E_i	E_f	R_{DCO} [c]	$J_i^\pi \rightarrow J_f^\pi$
18.8		18.8	0		
20.9		20.9	0		
54.3	8	339.3	285.0	0.66(5)	$10^+ \rightarrow 9^+$
58.7		58.7	0		
71.7	1	285.0	213.3		
154.6	7	213.3	58.7		
192.4	22	213.3	20.9	0.70(5)	
264.1	10	285.0	20.9	0.71(10)	
266.2	44	285.0	18.8	0.69(2)	
285.0	9	285.0	0		
318.4	100	339.3	20.9	0.63(2)	
339.3	16	339.3	0	0.80(5)	$10^+ \rightarrow 8^+$

[a]γ-ray energies are accurate to $\pm$0.3 keV.
[b]Errors are estimated to be less than 10% for the transitions with $I_\gamma > 10$ and less than 25% for the weaker ones. The values are normalized such that the one of the 318.4-keV transition is 100.
[c]Values when a gate is set on the 575.3-keV transition. The numbers in parentheses are the errors in the last digit.

IV. DISCUSSION

Low-lying states built on the 8^+ isomer in odd-odd ^{154}Ho are expected to be described by simple proton-neutron configurations involving the available single particle orbitals in the $Z = 64$ to 82 and $N = 82$ to 90 space. The 8^+ isomer could be interpreted as resulting from a high-K isomerism due to the coupling of a quasiproton particle and a quasineutron hole in the same intruder $h_{11/2}$ orbitals, namely, the $\pi h_{11/2}[532]5/2 \otimes \nu h_{11/2}[505]11/2$ configuration with $K = 5/2 + 11/2 = 8$ [22]. As we already mentioned in the previous section, the exact energy for the isomer has not been known but reported as to be 208 to 320 keV relative to the ground state [1,2,23]. Figure 6 shows a quasiparticle energy diagram for ^{154}Ho against quadrupole parameter ϵ_2 assuming no γ deformation. Here we adopted pairing parameters to be $\Delta_p = 1.13$ MeV for quasiprotons and $\Delta_n = 0.98$ MeV for quasineutrons, respectively [26]. Around $\epsilon_2 = 0.14$, the $h_{11/2}[523]7/2$, $h_{11/2}[532]5/2$, and $g_{7/2}[404]7/2$ orbitals for protons and the $f_{7/2}[532]3/2$ and $h_{9/2}[530]1/2$ orbitals for neutrons are favored energetically, and thus these proton-neutron combinations are expected to form low-lying states in ^{154}Ho. Accordingly, low-lying levels between the 8^+ isomer and the 10^+ at 339.3 keV can be interpreted as members of the multiplets resulting from one proton and one neutron based on the $\pi h_{11/2} \nu f_{7/2}$ and the $\pi h_{11/2} \nu h_{9/2}$ configurations. We notice that $J^\pi = 11/2^-$ based on the $\pi h_{11/2}$ orbital and $J^\pi = 7/2^-$ based on the $\nu f_{7/2}$ orbital consists of the ground state for ^{153}Ho [11] and for ^{153}Dy [9], respectively.

Bands 1 and 2, band 3, and band 4 are assigned configurations built on the $\pi h_{11/2} \nu i_{13/2}$, the $\pi h_{11/2} \nu h_{9/2}$, and the $\pi h_{11/2} \nu f_{7/2}$ alignments, respectively. These assignments

TABLE II. γ-ray energies, relative intensities, excitation energies, DCO ratios, and spin-parity assignments for the levels placed above the 10^+ at 339.3 keV in ^{154}Ho. The relative intensities are deduced from a sum spectrum gated on 192-, 264-, 266-, 285-, and 318-keV transitions and normalized such that the one of the 182.4 keV is 100. The electron conversion effect was not considered.

E_γ [a]	I_γ [b]	E_i [c]	E_f [c]	R_{DCO} [d]	$J_i^\pi \rightarrow J_f^\pi$
83.1		2385.4	2302.3		$18^- \rightarrow 17^-$
101.4		1198.4	1097.0		
136.2		5349.0	5212.8		$(25^+) \rightarrow (24^+)$
180.0		701.7	521.7		
182.4	100	521.7	339.3	0.71(1)	$11^- \rightarrow 10^+$
185.6	5	3640.4	3454.8	0.53(3)	$(21^+) \rightarrow (20^+)$
198.4		2385.4	2187.0	0.56(10)	$18^- \rightarrow (16^-)$
216.3		2446.2	2229.9		$(16^+) \rightarrow 16^+$
220.8		5436.7	5215.9	1.14(8)	$27^- \rightarrow 25^-$
252.3		2439.3	2187.0	0.85(8)	
265.1	1.5	5436.7	5171.6	0.96(12)	$27^+ \rightarrow 25^+$
279.2	18	1376.2	1097.0	0.66(3)	$14^- \rightarrow 13^-$
282.8		5212.8	4930.0		$(24^+) \rightarrow (24^+)$
286.4	21	1973.4	1687.0	0.68(2)	$16^- \rightarrow 15^-$
292.5	14	814.2	521.7	0.70(6)	$12^- \rightarrow 11^-$
324.2	0.1	3396.6	3072.4	0.74(15)	$20^- \rightarrow 19^-$
339.4	2	2641.7	2302.3	0.61(6)	$18^- \rightarrow 17^-$
346.2	1	4760.3	4414.1	0.56(20)	$24^- \rightarrow 23^-$
356.2	24	2741.6	2385.4	0.69(2)	$19^- \rightarrow 18^-$
358.7	1	3997.1	3638.4	0.55(25)	$22^- \rightarrow 21^-$
377.2	1	4930.0	4552.8	0.76(8)	$(24^+) \rightarrow (23^+)$
384.2	0.6	1198.4	814.2		
392.9	1	1868.5	1475.6	1.03(10)	$(14^+) \rightarrow 14^+$
412.0	38	2385.4	1973.4	0.99(1)	$18^- \rightarrow 16^-$
430.4	1.8	4070.8	3640.4	0.56(7)	$(22^+) \rightarrow (21^+)$
455.6	0.8	5215.9	4760.3	0.70(25)	$25^- \rightarrow 24^-$
456.9		2439.3	1973.4		
458.6	1	2187.0	1728.4		
475.8		3217.4	2741.6	0.73(8)	$20^- \rightarrow 19^-$
492.2		6351.9	5859.7		
496.7		1198.4	701.7		
500.0	3	2187.0	1687.0	0.78(7)	$(16^-) \rightarrow 15^-$
510.7		5859.7	5349.0	0.78(10)	$(26^+) \rightarrow (25^+)$
551.1	11	890.4	339.3	1.06(5)	$12^+ \rightarrow 10^+$
561.9		5998.6	5436.7	0.64(10)	$28 \rightarrow 27^-$
562.0	10	1376.2	814.2	1.00(3)	$14^- \rightarrow 12^-$
569.1	5	854.1	285.0	0.83(10)	$11^+ \rightarrow 9^+$
571.6		7453.9	6882.3	1.03(15)	$32 \rightarrow 30$
575.3	77	1097.0	521.7	1.01(1)	$13^- \rightarrow 11^-$
585.2	6	1475.6	890.4	0.99(3)	$14^- \rightarrow 12^+$
590.0	48	1687.0	1097.0	1.02(1)	$15^- \rightarrow 13^-$
597.2	17	1973.4	1376.2	1.01(2)	$16^- \rightarrow 14^-$
599.7	5	1453.8	854.1	1.01(5)	$13^+ \rightarrow 11^+$
615.3	11	2302.3	1687.0	0.98(2)	$17^- \rightarrow 15^-$
646.9		5859.7	5212.8	0.84(30)	$(26^+) \rightarrow (24^+)$
660.0		5212.8	4552.8	0.75(21)	$(24^+) \rightarrow (23^+)$
668.3	2	2641.7	1973.4	0.98(12)	$18^- \rightarrow 16^-$
676.7	1	1198.4	521.7		
687.0		3072.4	2385.4	0.55(40)	$19^- \rightarrow 18^-$
713.2	11	3454.8	2741.6	0.54(2)	$(20^+) \rightarrow 19^-$
754.3	2	2229.9	1475.6	1.01(10)	$16^+ \rightarrow 14^+$
754.9	1	3396.6	2641.7	0.88(9)	$20^- \rightarrow 18^-$

TABLE II. (*Continued*.)

E_γ [a]	I_γ [b]	E_i [c]	E_f [c]	R_{DCO} [d]	$J_i^\pi \rightarrow J_f^\pi$
757.5	3	5171.6	4414.1	0.91(7)	$25^- \rightarrow 23^-$
763.2	0.6	4760.3	3997.1	0.98(30)	$24^- \rightarrow 22^-$
770.1	2	3072.4	2302.3	0.92(7)	$19^- \rightarrow 17^-$
775.7	5	4414.1	3638.4	0.88(5)	$23^- \rightarrow 21^-$
777.4	1	3849.8	3072.4	0.88(5)	$21^- \rightarrow 19^-$
779.7	1	3997.1	3217.4	0.87(10)	$22^- \rightarrow 20^-$
782.6	1	4632.4	3849.8	0.89(12)	$23^- \rightarrow 21^-$
796.2	0.5	5349.0	4552.8	1.23(35)	$(25^+) \rightarrow (23^+)$
810.8	2	2187.0	1376.2	1.07(8)	$(16^-) \rightarrow 14^+$
816.2	1	3458.0	2641.7	0.85(7)	$20^- \rightarrow 18^-$
816.6		2270.4	1453.8	1.23(35)	$15^+ \rightarrow 13^+$
828.4	2	3058.3	2229.9	1.02(7)	$18^+ \rightarrow 16^+$
832.0	0.3	3217.4	2385.4		$20^- \rightarrow 18^-$
841.8	2	4299.8	3458.0	1.01(8)	$22^- \rightarrow 20^-$
859.2	0.3	4930.0	4070.8	0.95(35)	$(24^+) \rightarrow (22^+)$
883.7		6882.3	5998.6	1.20(15)	$30 \rightarrow 28$
896.8	9	3638.4	2741.6	0.93(3)	$21^- \rightarrow 19^-$
912.4	2.7	4552.8	3640.4	1.15(7)	$(23^+) \rightarrow (21^+)$
940.0		3169.9	2229.9	1.06(35)	$(18^+) \rightarrow 16^+$
970.6		2446.2	1475.6	1.10(35)	$(16^+) \rightarrow 14^+$
978.1		1868.5	890.4	0.88(26)	$(14^+) \rightarrow 12^+$
1018.1		6454.8	5436.7		
1072.6	2	3458.0	2385.4	0.93(6)	$20^- \rightarrow 18^-$
1240.3		6677.0	5436.7	0.92(20)	$27^- \rightarrow (29^-)$

[a] γ-ray energies are accurate to ± 0.3 keV.
[b] Errors are estimated to be less than 15% for the transitions with $I_\gamma > 10$ and less than 30% for the weaker ones. The values are normalized such that the one of the 184.4-keV transition is 100. Blanks indicate weak intensities less than 0.5.
[c] Energies are relative to the 8^+ isomer.
[d] Values when gates are set on a stretched quadrupole transition. The numbers in parentheses are the errors in the last digit.

are consistent with the single particle bands established in the neighboring odd-proton ^{153}Ho and odd-neutron ^{153}Dy nuclei. Bands 3 and 4 are fully aligned ones, as $\pi h_{11/2} \nu h_{9/2}$ for even spins and $\pi h_{11/2} \nu f_{7/2}$ for odd spins, respectively, which were also observed in ^{152}Tb [24,25], thus giving rise to bandhead spins of 10 and 9. The present spin assignments

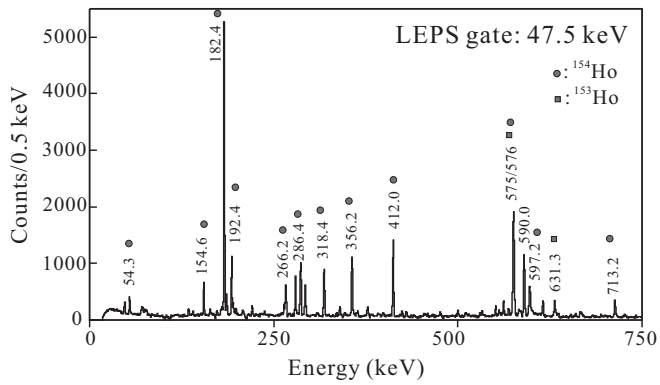

FIG. 3. Coincidence γ-ray spectrum gated set on the 47-keV Ho $K\alpha_1$ x ray. Circles (rectangles) at peaks represent characteristic γ rays for ^{154}Ho (^{153}Ho).

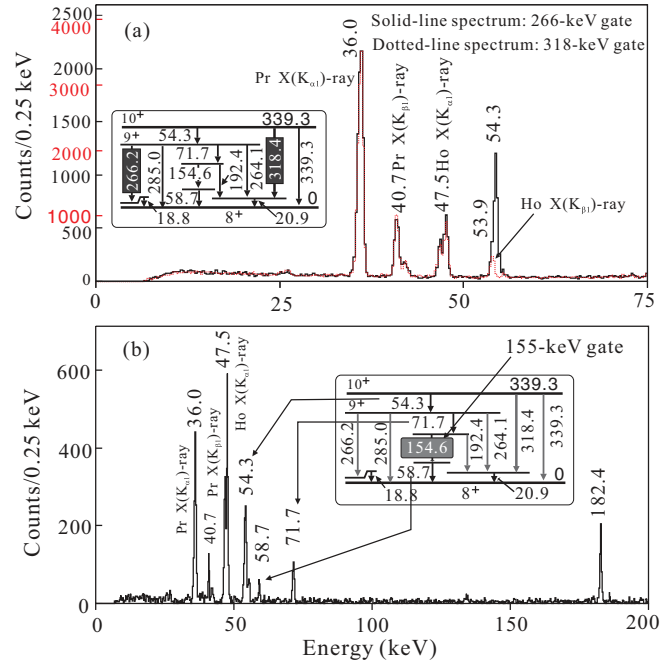

FIG. 4. (Color online) (a) Two overlapping LEPS spectra in coincidence with the 266-keV transition and the 318-keV transition, respectively, and (b) a LEPS spectrum when gating the 155-keV transition. For clarity, the corresponding level schemes are inserted.

for the bandheads are also consistent with the systematics of the bands observed in heavier odd-odd Ho isotopes [16–19]. Figure 7 shows a systematic trend for the band of ^{154}Ho and the band of ^{153}Ho [11] together with ^{152}Dy [4] and ^{154}Dy [5] core states. As evident in this figure, the level structure based on the $\pi h_{11/2} \nu i_{13/2}$ and the $\pi h_{11/2}$ configurations exhibit a vibrational-like character rather than a rotational one. It means that the level structure of ^{154}Ho based on the intruder proton $h_{11/2}$ orbital and the intruder neutron $i_{13/2}$ orbital follows the systematics of neighboring nuclei core states with $N = 86$. Such a dominance of the neutron $N = 86$ for the structure of ^{154}Ho becomes more clear by comparing to the ground band of ^{154}Er ($N = 86$) [6] as seen in Fig. 8.

At higher spins, the behavior of the level structure exhibits more complexity, showing shape coexistence of collective and noncollective states due to competition between a collective quadrupole band and quasiparticle aligned configuration. In Fig. 9(a), we show the experimental level energies at a given angular momentum for bands 1 to 4 and yrast states (the lowest energy levels at a given angular momentum), and in Fig. 9(b) the relative excitation energies in the form of rigid rotor plots where a rotating liquid-drop energy reference equal to $(\hbar^2/2I_{rig})J(J+1)$, where $I_{rig} = (2/5)\ AMR^2$ has been subtracted. Here A, M, and R are mass number, atomic mass, and nuclear radius, respectively. As far as collective level structures are concerned, the band energy spacings in ^{154}Ho deviate from a typical rotational-like $\Delta J = 2$ sequence. Nevertheless, excitation energies given in the form of a rigid rotor reference are very useful for studying aligned particle yrast structures in a small deformed nucleus. Actually for small deformations, both terminating rotational bands

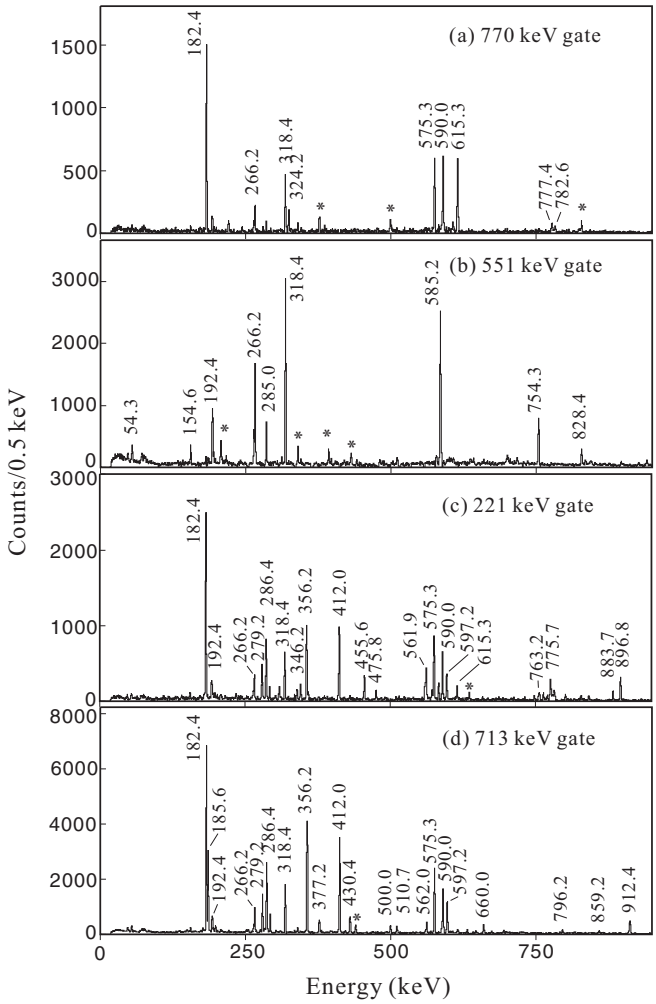

FIG. 5. Representative spectra (a) for showing transitions in band 1 when gating the 770-keV transition, (b) for the transitions in band 3 when gating the 551-keV transition, (c) for the transitions in Group 1 when gating the 221-keV transition, and (d) for the transitions in Group 2 when gating the 713-keV transition. Peaks with an asterisk indicate contaminants from other nuclei.

and strongly collective bands are obtained in the rotating harmonic oscillator, and thus all bands gradually approach the noncollective limit with maximum spin alignment in a state of pure particle-hole nature [27,28].

As Fig. 9(b) shows, the 18^-, the 19^-, and the 27^- states are unusually lower in energy. Such energetically favored states have been also observed in the neighboring ^{152}Dy, ^{153}Dy, and ^{153}Ho nuclei. For example, in ^{152}Dy [4] the 8^+ at 2437 keV, the 11^- with $T_{1/2} = 3.9$ ns at 3160 keV, the 17^+ with $T_{1/2} = 60$ ns at 5088 keV, and the 21^- with $T_{1/2} = 10$ ns at 6127 keV are known to be energetically favored states formed by aligned multiparticle configurations. The 8^+ state with $T_{1/2} = 10$ ps in ^{152}Dy has been interpreted as being a noncollective oblate state associated with two-neutron $[\nu(f_{7/2}h_{9/2})]_{8^+}$ alignment [4]. The corresponding energetically favored state in ^{153}Ho [11] is also found at $J^\pi = 27/2^-$ as shown in Fig. 7, which is associated with the coupling of the proton $h_{11/2}$ orbital to the $[\nu(f_{7/2}h_{9/2})]_{8^+}$ configuration. Thereby the energetically

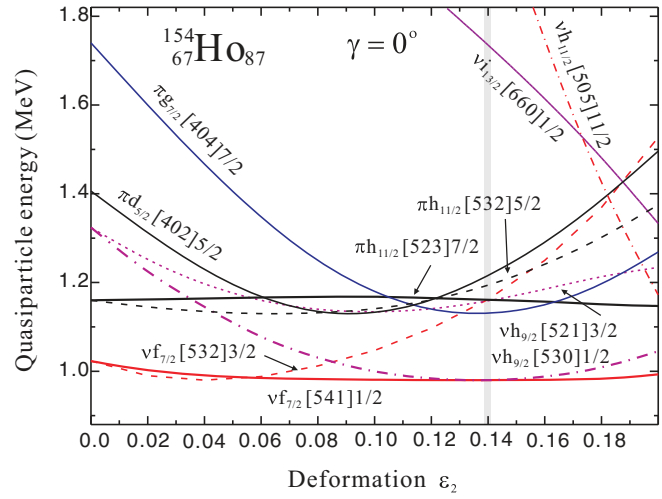

FIG. 6. (Color online) Calculated proton and neutron quasiparticle energy diagram for ^{154}Ho as a function of quadrupole deformation parameter ϵ_2 at $\gamma = 0^o$. The used pairing parameters are $\Delta_p = 1.13$ MeV for quasiprotons and $\Delta_n = 0.98$ MeV for quasineutrons. The Nilsson orbitals are labeled by the asymptotic quantum number $[N, n_z, \Lambda]\Omega$. See text for more details.

favored 18^- and the 19^- states in odd-odd ^{154}Ho could be interpreted as being associated with the coupling of the $\pi h_{11/2}\nu i_{13/2}$ configuration to the said 8^+ state in ^{152}Dy, and thus we suggest that the 19^- level is a noncollective oblate state formed by the four quasiparticle full alignment $[\pi(h_{11/2})\nu(f_{7/2}h_{9/2}i_{13/2})]_{19^-}$. It should be noted that the $\nu f_{7/2}[532]3/2$ and the $\nu h_{9/2}[530]1/2$ orbitals are almost degenerate at $\epsilon_2 = 0.13$ to 0.15 keeping the lowest energy trajectories as seen in Fig. 6. As Fig. 9(b) shows, the unusually low-lying 27^- state is noticeable. Taking into account an excitation energy and a spin value, the 27^- level can be interpreted as a result of six-quasiparticle alignment. According to cranked shell model (CSM) calculations, the $\pi h_{11/2}$ orbitals are found to be easily aligned with increasing angular velocity. Thus we propose that four $E2$ transitions between the 27^- and the 19^- levels are largely the $[\pi(h_{11/2})^3]\otimes[\nu(f_{7/2}h_{9/2}i_{13/2})]$ configuration with the $h_{11/2}$ proton pair contributing 0^+ to 8^+ spins. Thereby the energetically favored 27^- level is most

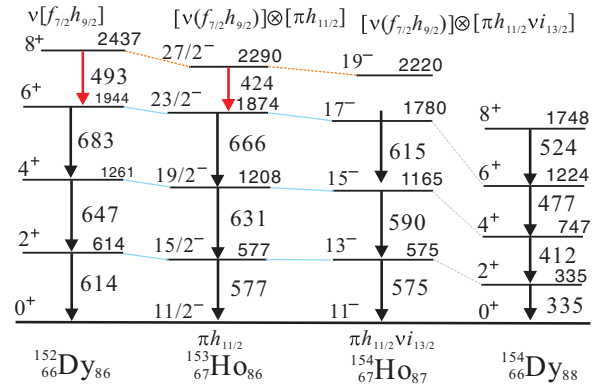

FIG. 7. (Color online) Level systematics of the yrast states for ^{152}Dy [4], ^{153}Ho [11], ^{154}Ho, and ^{154}Dy [5].

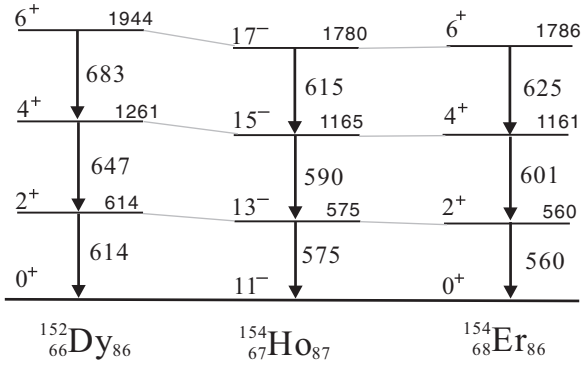

FIG. 8. Systematics for the yrast states in ^{152}Dy [4], ^{154}Ho, and ^{154}Er [6].

likely a noncollective state associated with a six-quasiparticle alignment, namely, $[\pi(h_{11/2})^3]_{27/2^-}\otimes[\nu(f_{7/2}h_{9/2}i_{13/2})]_{27/2^-}$. This state could be also understood as arising from the $\pi h_{11/2}\nu i_{13/2}$ alignment coupled to the low-lying energy level at 17^+ based on the $[\pi(h_{11/2})^2]\otimes[\nu(f_{7/2}h_{9/2})]$ configuration in ^{152}Dy (see Fig. 10).

The excited states labeled Group 2 suggest apparently single-particle level structures as seen in Fig. 11. In order to explore in further details the level properties, we performed

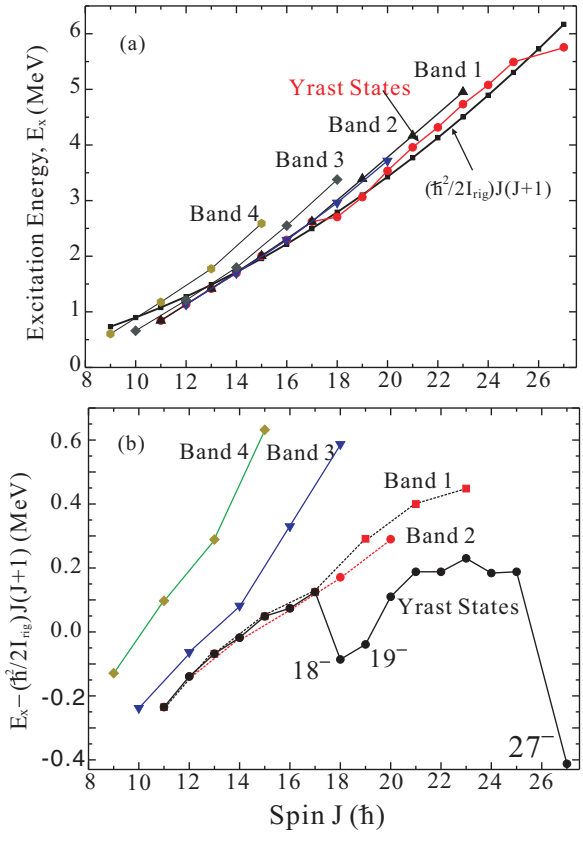

FIG. 9. (Color online) Excitation energy versus spin J for bands 1 to 4 and yrast states in ^{154}Ho. For comparison an average liquid-drop energy, $(\hbar^2/2I_{\rm rig})J(J+1)$, is given in (a) while in (b) excitation energy relative to a liquid-drop energy for the states is given. Here $\hbar^2/2I_{\rm rig} = 0.00812$ MeV.

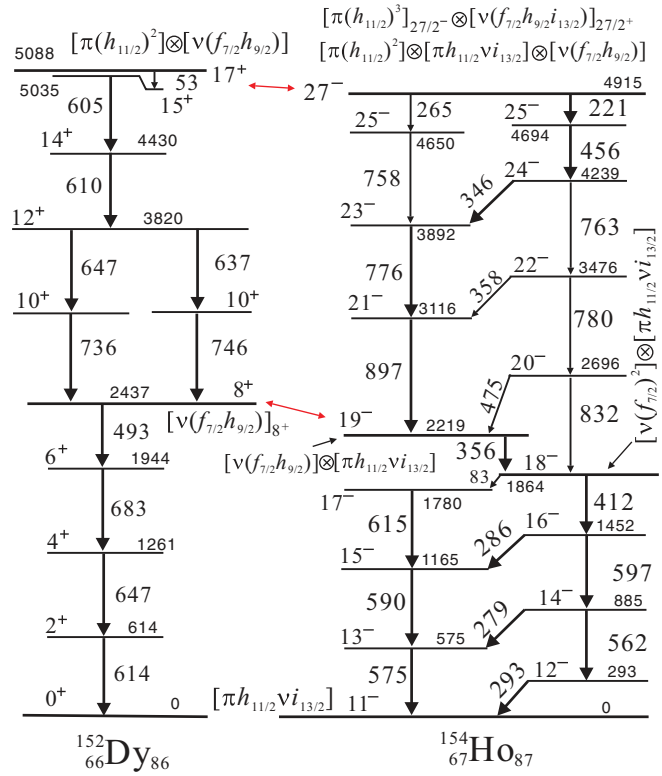

FIG. 10. (Color online) Comparison between the yrast states in ^{152}Dy [4] and ^{154}Ho. The energetically favored states are denoted by the correspondingly aligned quasiparticle configurations.

a calculation for single quasiparticle energies against ϵ_2 at $\gamma = 60^o$ and compared the results with those obtained at $\gamma = 0^o$. We found that there is the high probability of

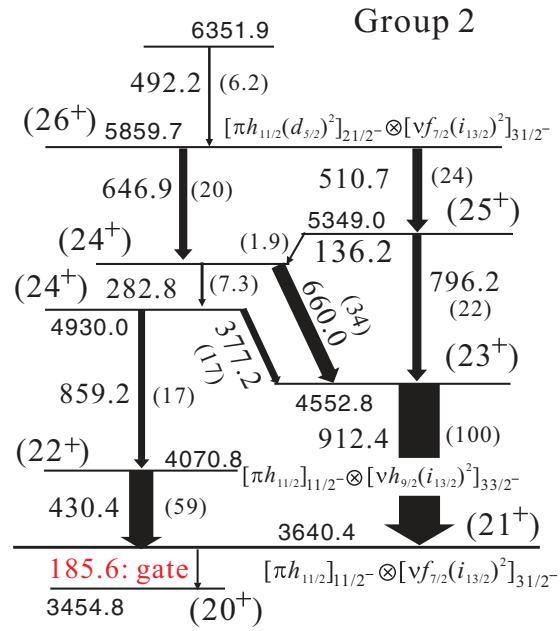

FIG. 11. (Color online) Expanded level scheme for Group 2 states feeding the 21^+ level at 3640.4 keV. The relative intensities of the γ-ray transitions are deduced from a 185.6-keV gate spectrum and are normalized such that the one of the 912.4-keV transition is 100.

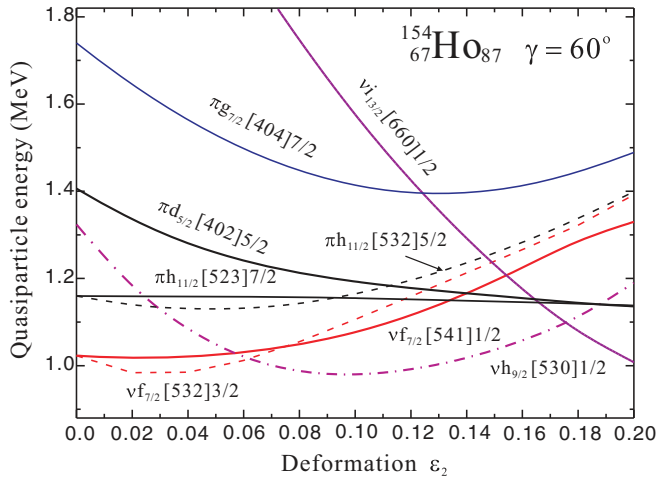

FIG. 12. (Color online) Calculated proton and neutron quasiparticle energies for ^{154}Ho as a function of quadrupole deformation parameter ε_2 at $\gamma = 60^{\circ}$. The used pairing parameters are $\Delta_p = 1.13$ MeV for quasiprotons and $\Delta_n = 0.98$ MeV for quasineutrons. The Nilsson orbitals are labeled by the asymptotic quantum number $[N, n_z, \Lambda]\Omega$.

populating the $\nu i_{13/2}[660]1/2$ and the $\pi d_{5/2}[402]5/2$ orbitals as seen in Fig. 12 and thus noncollective oblate states due to their alignments are also expected. Furthermore, the $\nu i_{13/2}[660]1/2$ orbital has a sharp down slope with a large spin alignment against angular velocities. Accordingly, a most likely candidate for the 21^+ level structure is a four-quasiparticle configuration consisting of a pair of neutrons in the intruder $i_{13/2}$ orbital coupled to the $\pi h_{11/2}\nu f_{7/2}$ configuration. This four-quasiparticle configuration agrees well with a maximum angular momentum $J^{\pi} = 21^+$ based on the full $[\pi h_{11/2}]_{11/2^-} \otimes [\nu f_{7/2}(i_{13/2})^2]_{31/2^-}$ alignment. Given the $[\pi h_{11/2}] \otimes [\nu h_{9/2}(i_{13/2})^2]$ configuration for the 21^+ level, the 22^+ level at 4070.8 keV can be interpreted as being based on the four-quasiparticle $[\pi h_{11/2}]_{11/2^-} \otimes [\nu h_{9/2}(i_{13/2})^2]_{33/2^-}$ alignment. Here we would like to point out that the intensity of the 430.4-keV γ ray is much larger than that of the 859.2 keV γ ray as denoted in Fig. 11. Such an unbalanced intensity between the populating and the depopulating transitions implies that the 22^+ level may be an isomer with a half-life of a few hundreds of ns.

Finally, we concentrate on the 26^+ level at 5859.7 keV which is an energetically favored state as well. We propose that the states of 23^+ to 26^+ should be associated with a six-quasiparticle excitation consisting of a pair of protons in the orbital $\pi d_{5/2}[402]5/2$ coupled to the aligned $[\pi h_{11/2}] \otimes [\nu f_{7/2}(i_{13/2})^2]$ configuration. Thus the 26^+ level could be interpreted as a noncollective oblate state based on the fully aligned $[\pi h_{11/2}(d_{5/2})^2]_{21/2^-} \otimes [\nu f_{7/2}(i_{13/2})^2]_{31/2^-}$ configuration. The γ-ray transitions above the energetically favored 27^- and 26^+ states appear to be associated with core-breaking excitations. However, detailed microscopic calculations are required to ascertain the above interpretation of the energetically favored terminating states.

V. CONCLUSION

We presented extensive new experimental information about the level scheme of the odd-odd ^{154}Ho. Through the use of a LEPS Ge detector, we have clearly established the complicated low-lying energy transitions just above the 3.10 min isomer and extended the known levels to higher spins. The level structures were discussed in the light of the known systematics of neighboring Dy, Eb, and odd-mass Ho states. The collective bands built on proton-neutron two configurations, such as $\pi h_{11/2}\nu i_{13/2}$, $\pi h_{11/2}\nu h_{9/2}$, and $\pi h_{11/2}\nu f_{7/2}$, exhibit vibrational character similar to that seen in core states of Dy and Er with $N = 86$ rather than rotational character in the neighboring nuclei with $N = 88$.

Several yrast noncollective states where the nuclear spin made up completely from single-particle angular momentum contributions have been identified. An energetically favored state $J^{\pi} = 19^-$ could be interpreted as being attributed to the coupling of the $\pi h_{11/2}\nu i_{13/2}$ orbital to the yrast 8^+ state in neighboring core ^{152}Dy, namely, four-quasiparticle full alignment of the $[\pi h_{11/2}\nu i_{13/2}]_{11^-} \otimes [\nu(h_{9/2}f_{7/2})]_{8^-}$ configuration. Another energetically favored state $J^{\pi} = 27^-$ was thought to be associated with a six-quasiparticle alignment, namely, $[\pi(h_{11/2})^3]_{27/2^-} \otimes [\nu(f_{7/2}h_{7/2}i_{13/2})]_{27/2^-}$. The 21^+ and the 26^+ states with positive-parity were assigned to noncollective oblate states built on the four-quasiparticle $[\pi h_{11/2}] \otimes [\nu f_{7/2}(i_{13/2})^2]$ and the six-quasiparticle $[\pi h_{11/2}(d_{5/2})^2]_{21/2^-} \otimes [\nu f_{7/2}(i_{13/2})^2]_{31/2^-}$ configurations, respectively.

ACKNOWLEDGMENT

This research was supported by the Academic Research fund of Hoseo University in 2012.

[1] *Table of Isotopes*, 8th ed., edited by R. B. Firestone and V. S. Shirley (Wiley, New York, 1996), and references therein.
[2] National Nuclear Data Center, Brookhaven National Laboratory, http://www.nndc.bnl.gov/nudat2/
[3] R. F. Casten, D. D. Warner, D. S. Brenner, and R. L. Gill, Phys. Rev. Lett. **47**, 1433 (1981).
[4] J. Styczen, Y. Nagai, M. Piiparinen, A. Ercan, and P. Kleinheinz, Phys. Rev. Lett. **50**, 1752 (1983).
[5] W. C. Ma, M. A. Quader, H. Emling, T. L. Khoo, I. Ahmad, P. J. Daly, B. K. Dichter, M. Drigert, U. Garg, Z. M. Grabowski, R. Holzmann, R. V. F. Janssens, M. Piiparinen, W. H. Trzaska, and T. F. Wang, Phys. Rev. Lett. **61**, 46 (1988).
[6] M. H. Rafailovich, O. C. Kistner, A. W. Sunyar, S. Vajda, and G. D. Sprouse, Phys. Rev. C **30**, 169 (1984).
[7] R. B. Cakirli and R. F. Casten, Phys. Rev. C **78**, 041301(R) (2008).

[8] G. A. Lalazissis, S. Raman, and P. Ring, At. Data Nucl. Data Tables **71**, 1 (1999).
[9] M. Kortelahti, R. Broda, Y. H. Chung, P. J. Daly, H. Helppi, J. McNeill, A. Pakkanen, P. Chowdhury, R. V. F. Janssens, T. L. Khoo, and W. Kuhn, Phys. Lett. B **131**, 305 (1983).
[10] N. Nica *et al*., Phys. Rev. C **64**, 034313 (2001).
[11] D. C. Radford, M. S. Rosenthal, P. D. Parker, J. A. Cizewski, J. H. Thomas, B. Haas, F. A. Beck, T. Byrski, J. C. Merdinger, A. Nourredine, Y. Schutz, J. P. Vivien, J. S. Dionisio, and Ch. Vieu, Phys. Lett. B **126**, 24 (1983).
[12] G. B. Hagemann, J. D. Garrett, B. Herskind, J. Kownacki, B. M. Nyakó, P. L. Nolan, and J. F. Sharpey-Schafer, Nucl. Phys. A **424**, 365 (1984).
[13] A. Piepke, N. Mansour, A. Moussavi, H. Sanchez, H. Strecker, K. Grotz, J. Metzinger, and H. V. Klapdor, Nucl. Phys. A **486**, 335 (1988).
[14] D. E. Appelbe, P. J. Twin, C. W. Beausang, D. M. Cullen, D. Curien, G. Duchene, S. Erturk, C. Finck, B. Haas, E. S. Paul, D. C. Radford, C. Rigollet, M. B. Smith, O. Stezowski, J. C. Waddington, and A. N. Wilson, Phys. Rev. C **66**, 044305 (2002).
[15] S. J. Chae, J. C. Kim, C. S. Lee, C.-B. Moon, T. Komatsubara, J. Mukai, J. Lu, T. Hayakawa, M. Matsuda, T. Watanabe, and K. Furuno, Z. Phys. A **350**, 89 (1994).
[16] S. H. Bhatti, J. C. Kim, S. J. Chae, J. H. Ha, C. S. Lee, J. Y. Moon, C.-B. Moon, T. Komatsubara, J. Lu, M. Matsuda, T. Hayakawa, T. Watanabe, and K. Furuno, Z. Phys. A **353**, 119 (1995).
[17] D. M. Cullen, C.-H. Yu, D. Cline, M. Simon, D. C. Radford, M. A. Riley, and J. Simpson, Phys. Rev. C **57**, 2170 (1998).
[18] J. Lu, Y. Liu, X. Wu, Y. Ma, G. Zhao, H. Sun, J. Huo, S. Wen, G. Li, and C. Yang, Phys. Rev. C **59**, 3461 (1999).
[19] D. Escrig, A. Jungclaus, B. Binder, A. Dietrich, T. Härtlein, H. Bauer, Ch. Gund, D. Pansegrau, D. Schwalm, D. Bazzacco, G. de Angelis, E. Farnea, A. Gadea, S. Lunardi, D. R. Napoli, C. Rossi Alvarez, and C. A. Ur, Eur. Phys. J. A **21**, 67 (2004).
[20] C. Baktash, in *Proceedings of the Conference on High Angular Momentum Properties of Nuclei, Oak Ridge, 1982* (Harwood Academic, New York, 1983), p. 207.
[21] Balraj Singh, Nucl. Data Sheets **110**, 1 (2009).
[22] A. K. Jain, R. K. Sheline, D. M. Headly, P. C. Sood, D. G. Burke, I. Hrivnacova, J. Kvasil, D. Nosek, and R. W. Hoff, Rev. Mod. Phys. **70**, 844 (1998).
[23] G. Audi, O. Bersillon, J. Blachot, and A. H. Wapstra, Nucl. Phys. A **729**, 3 (2003).
[24] Agta Artna-Cohen, Nucl. Data Sheets **79**, 1 (1996).
[25] D. Barneoud, J. A. Pinston, C. Foin, and E. Monnand, Z. Phys. A **314**, 69 (1983).
[26] P. Möller, J. R. Nix, and K.-L. Kratz, At. Data Nucl. Data Tables **66**, 131 (1997).
[27] I. Ragnarsson, Phys. Lett. B **199**, 317 (1987).
[28] I. Ragnarsson *et al*., Phys. Scr. **34**, 651 (1986).